

Comprehensive Characterization of InGaAs/InP Avalanche Photodiodes at 1550 nm with an Active Quenching ASIC

Jun Zhang, Rob Thew, Jean-Daniel Gautier, Nicolas Gisin, and Hugo Zbinden

Abstract—We present an active quenching application specific integrated circuit (ASIC), for use in conjunction with InGaAs/InP avalanche photodiodes (APDs), for 1550 nm single-photon detection. To evaluate its performance, we first compare its operation with that of standard quenching electronics. We then test 4 InGaAs/InP APDs using the ASIC, operating both in the free-running and gated modes, to study more general behavior. We investigate not only the standard parameters under different working conditions but also parameters such as charge persistence and quenching time. We also use the multiple trapping model to account for the afterpulsing behavior in the gated mode, and further propose a model to take account of the afterpulsing effects in the free-running mode. Our results clearly indicate that the performance of APDs with an on-chip quenching circuit significantly surpasses the conventional quenching electronics, and makes them suitable for practical applications, e.g., quantum cryptography.

Index Terms—Avalanche photodiodes (APDs), SPAD, single-photon detection, telecom wavelengths, ASIC, quantum cryptography.

I. INTRODUCTION

Single-photon detectors are the key components in numerous photonics-related applications such as quantum cryptography [1], optical time domain reflectometry [2], [3] and integrated circuit testing [4]. We can classify single-photon detection into four classes: photomultiplier tubes [5]; semiconductor APDs [6], [7]; superconducting detectors [8]; and novel proposals such as using a single-electron transistor consisting of a semiconductor quantum dot [9]. In the telecommunication regime (1550 nm), InGaAs/InP APDs are currently the best choice for practical applications such as quantum cryptography [1] due to their favorable characteristics such as cost, size and robust operation with only thermo-electric cooling required.

To detect single photons, APDs must work in the so-called Geiger mode in which an inverse bias voltage (V_{bv}), exceeding the breakdown voltage (V_{br}), is applied, such that even a single photoexcited carrier (electron-hole pair) can create a persistent avalanche and a subsequent macroscopic current pulse due to the process of impact ionization. After the avalanche, a passive or active quenching circuit [6], is used to reduce V_{bv} down to below V_{br} , output a synchronized pulse and reset the APD for detecting the next photon.

Manuscript received. This work was supported by the Swiss NCCR Quantum Photonics and the Swiss CTI.

J. Zhang, R. Thew, J.-D. Gautier, N. Gisin, and H. Zbinden are with the Group of Applied Physics, University of Geneva, 1211 Geneva 4, Switzerland e-mail: (Jun.Zhang@unige.ch).

InGaAs/InP APDs are currently fabricated with separate absorption, charge and multiplication layers [7] to ensure the lattice matching and preserve a low electric field in the InGaAs absorption layer with a narrower bandgap ($E_g = 0.75$ eV for $\text{In}_{0.53}\text{Ga}_{0.47}\text{As}$), minimizing the induced leakage currents, while a high electric field in the InP multiplication layer, enhancing the impact ionization effect. The middle charge layer can efficiently control the electric field profiles of the absorption and multiplication layers. The parameters of APDs are affected by many factors such as the crystalline quality of semiconductor device, imperfections of design and fabrication, quenching circuit, and operational conditions. Therefore, actual performance of these APDs is always compromised and optimized for different applications.

In the past decade efforts have been made to characterize and further improve APD performance on the single-photon level at 1550 nm [10]–[22]. Recently, integration of the quenching electronics for InGaAs/InP APDs to an ASIC [23], [24] has been implemented. The measured results on some key parameters of APDs demonstrate active quenching ASICs can efficiently improve the noise-efficiency performance, and it has been shown that these APDs can work in a free-running mode [24]. However, full characterization of APDs with the ASIC is still necessary to better understand the improvements they provided. In this paper, we fully test 4 InGaAs/InP APDs at 1550 nm with an active quenching ASIC operating both in the free-running and gated modes, and compare the improvements with conventional electronics.

II. THE SETUP AND THE PRINCIPLE OF THE ASIC

The schematic setup for testing APDs is shown in Fig. 1. A digital delay pulse generator (DG 535, Stanford Research Systems Inc.) provides synchronous signals for the whole system. One of its periodic outputs drives a 1550 nm laser diode (LD) to produce short optical pulses with ~ 200 ps FWHM. The optical pulses are split into two parts by a 10/90 asymmetric fiber beamsplitter (BS). 90% of the signal is monitored by a power meter (IQ 1100, EXFO Co.) to regulate the precise variable attenuator (Var. ATT, IQ 3100, EXFO Co.) in real-time and stabilize the intensity of the output from the attenuator that goes to the pigtailed APD. The pins of the APD and ASIC are soldered together on a small printed circuit board, while the body of APD is fixed on the top of 4-layer thermoelectric cooler and actively stabilized with a closed-loop control.

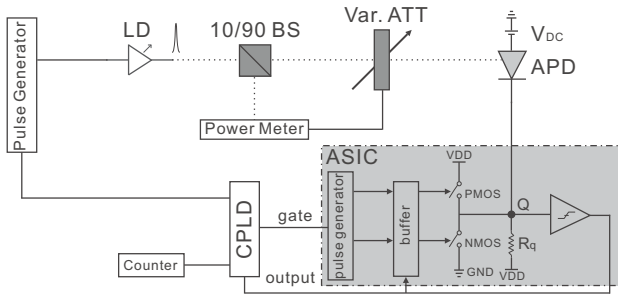


Fig. 1. The experimental setup.

The schematic diagram of the ASIC, fabricated with a $0.8\ \mu\text{m}$ complementary metal oxide semiconductor (CMOS) process, is shown in the gray area of Fig. 1. The amplitude of the gate signals from the complex programmable logic device (CPLD) is first converted to the power supply voltage VDD (+5 V) of the chip. Two pulses are then generated to control the PMOS and NMOS switches respectively which have extremely fast rise and fall times. There is a very short delay between the two control pulses to avoid the simultaneous conduction of the two switches. The timing is such that at the beginning of the gate the PMOS switch is closed while the NMOS switch is opened, to charge the voltage at the quenching point (Q) up to VDD, and then the PMOS switch is reopened. The total voltage difference between cathode and anode of the APD is $V_{bv} = \text{VDD} + |V_{DC}|$, exceeding V_{br} for Geiger mode operation. The NMOS switch remains open until the end of the gate if no avalanche happens, or until the active quenching after a triggered avalanche. During the avalanche process, current across the APD rapidly increases and results in an increasing voltage drop across the resistor R_q . The comparator and the following circuit quickly detects the the voltage drop at Q and immediately informs the buffer to close the NMOS switch to drop the voltage at Q to zero, and also generate a synchronous detection output to the CPLD. Normally the detector output maintains the high level until the falling edge of the next gate. Actually, when a detection is registered the CPLD inserts a short reset pulse after the gate, otherwise the CPLD does nothing. In the free-running mode, the gates from the CPLD are not used and VDD is applied to the cathode of the APD until an avalanche is excited. Further technical description about the ASIC can be found in Ref. [23].

III. PERFORMANCE TESTS OF APDS

We have tested 4 commercial APDs: #1 (JDSU0131T1897); #2 (JDSU0122E1711); and #3 (Epitaxx9951E9559) from JDSU; as well as #4 (PLI-DOI61910-040W059-076) from Princeton Lightwave, Inc., and compared the different performance characterizations of these APDs with the ASIC quenching system.

A. Integrated versus conventional quenching electronics

Firstly, we perform the key parameter measurements on the same (#3) APD using the new (ASIC) and old (conventional non-integrated circuit) [11], [14] quenching electronics under the same settings ($T = 223\ \text{K}$). Fig. 3 shows the comparison

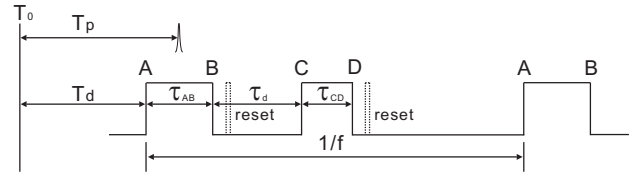


Fig. 2. The timing diagram for the afterpulse measurements using the double-gate method.

results for dark count (P_{DC} per ns) vs single-photon detection efficiency (P_{DE}) probabilities, afterpulse probability (P_{AP}) and jitter, respectively. Using the double-gate method [14] (we discuss this in the latter section) as shown in Fig. 2, these parameters can be related to:

$$P_{DC} = \frac{C_{DC}}{f\tau_{AB}}, \quad P_{AP} = \frac{C_{AP}}{C_{DE}\tau_{CD}}, \quad P_{DE} = \frac{1}{\mu} \ln \frac{1 - \frac{C_{DC}}{f}}{1 - \frac{C_{DE}}{f}}, \quad (1)$$

where C_{DC} (C_{AP} , C_{DE}) is the observed dark count (afterpulse, detection) rate, τ_{AB} (τ_{CD}) is the effective width of detection (afterpulse) gate in ns and μ is the mean photon number per optical pulse with repetition frequency of f . During the experiment, the conditions are $f = 10\ \text{kHz}$, $\tau_{AB} = \tau_{CD} = 100\ \text{ns}$ and $\mu = 1$, and these are fixed unless specifically mentioned in this paper.

The three curves manifestly exhibit the performance improvements provided by the new quenching electronics. The improvement of a factor of 3 in the P_{DC} - P_{DE} performance for #3 APD shown in Fig. 3a is better than expected. As we know, due to the ASIC the size of the electronics are greatly decreased and the electronic cables and the lengths of wires are reduced. This brings a lot of benefits such as superior signal integrity, minimized parasitic capacitance and reducing fake avalanche signals due to signal reflections or electronic noise. We also observe P_{DC} - P_{DE} performance improvements on other APDs, for instance, for #2 APD shown in Fig. 3a the ratio is always about 1 (no improvement) when $P_{DE} < 13\%$ and slowly increases to about 2 when $P_{DE} \sim 25\%$. The P_{DC} - P_{DE} performance improvement ratio strongly depends on the APD devices and operational conditions. Although the reasons of the significant improvement for #3 APD are not clear yet, one possibility could be different gate heights and discrimination approaches between the two quenching systems, as it is the noise that is improved here, for a given excess bias voltage.

We see, in Fig. 3b, a significant improvement in the P_{AP} between the two cases as expected. The P_{AP} is generally proportional to the total number of carriers generated during an avalanche and hence motivates small and rapidly quenched avalanches. The results here clearly illustrate the circuit response and quenching time of the new system for the avalanche discrimination are faster than the old system. We will come back to this in more details in the following sections.

Timing jitter (time resolution) is another key parameter. It is defined as the temporal uncertainty of detection output for an avalanche with fixed arrival time of photons. Time jitter strongly depends on device fabrication and P_{DE} , correspond-

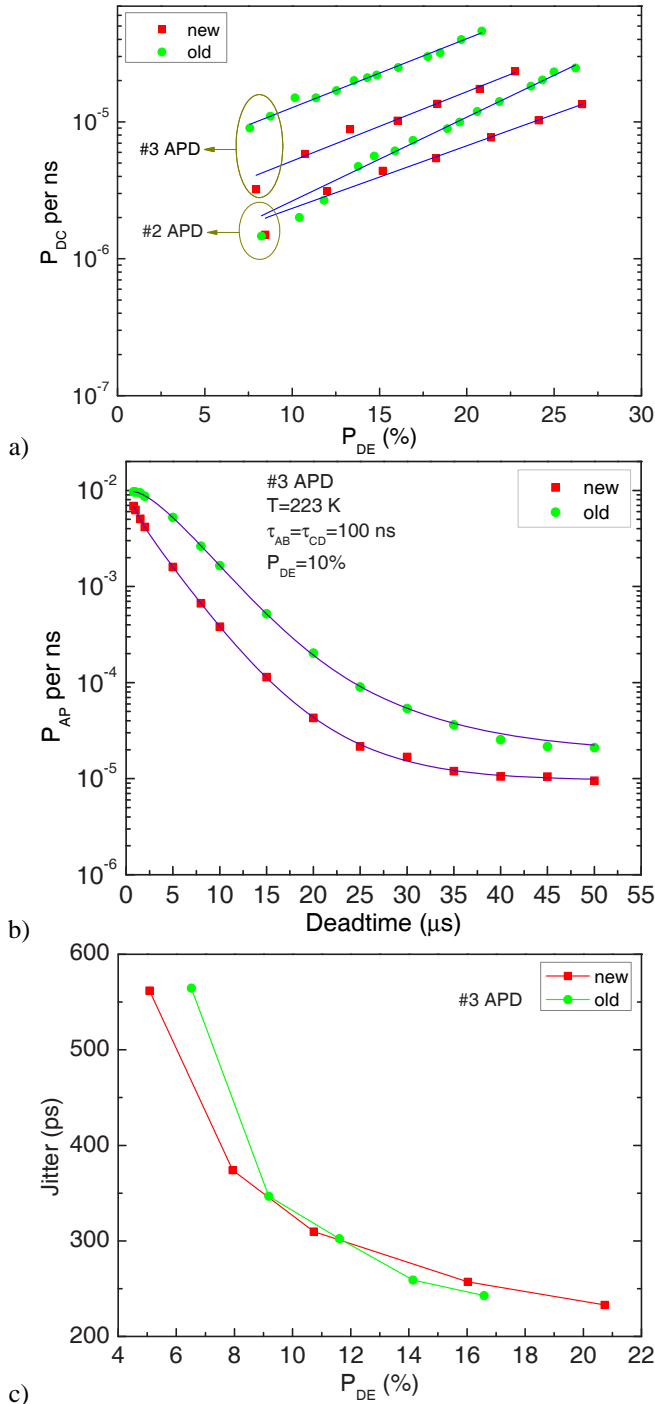


Fig. 3. a) Dark counts per ns (P_{DC}) versus detection efficiency (P_{DE}). b) Afterpulse probability per ns (P_{AP}) versus deadtime (τ_d). c) Time jitter versus P_{DE} .

ing to excess bias (V_{eb}) on the APD. Larger V_{eb} can generate higher electric fields, which will shorten the trapping time of the carriers in the absorption and grading layers, and also the buildup time of avalanche, hence reducing the jitter. To measure this we use a time-correlated single photon counting (TCSPC) board (SPC-130, Becker & Hickl GmbH) with a time resolution of 6 ps FWHM and minimum time slot of 815 fs, to measure the jitter properties. A synchronized signal from a pulse generator is used as the TCSPC's "stop" while

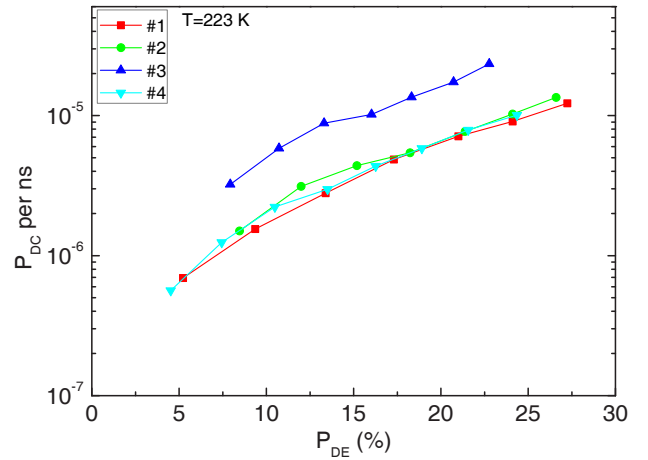


Fig. 4. P_{DC} versus P_{DE} of 4 APDs.

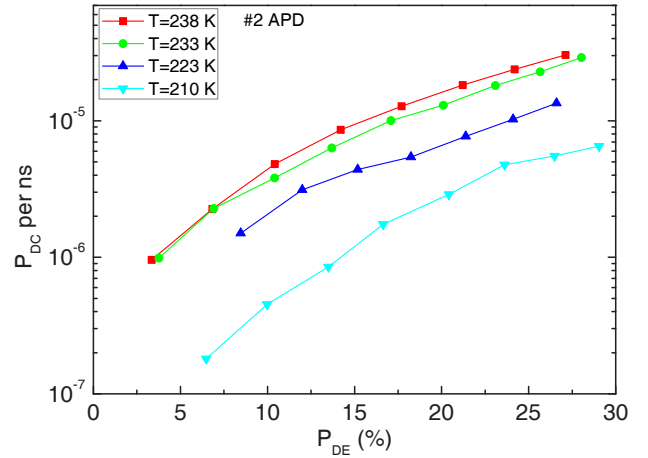


Fig. 5. P_{DC} versus P_{DE} of #2 APD at different T.

the detection output signal is used as "start". The measured jitter is the overall jitter of the system, including the jitter (< 60 ps) and width (~ 200 ps) of arrived optical pulses, the APD's intrinsic jitter owing to the stochastic process of carrier dynamics, as well as from the associated electronics. The jitter performance is shown in Fig. 3c and we only see a minor improvement when $P_{DE} < 10\%$. We expect the electronic jitter to be slightly better as the ASIC can efficiently reduce the propagation time and jitter of the signals. At higher P_{DE} we don't observe the improvement and the negligible difference between the two cases is due to contributions from the associated external electronics, e.g., CPLD and discriminator that are used with the new system but not the old one. However, varying degrees of improvement have been observed on other APDs even at higher P_{DE} .

B. P_{DC} , P_{DE} and thermal activation energy

In order to illustrate the universal improvements afforded by this new quenching system, we use the new system operating in the gated mode to repeat the measurement on different APDs and temperature settings, as shown in Fig. 4 and Fig. 5.

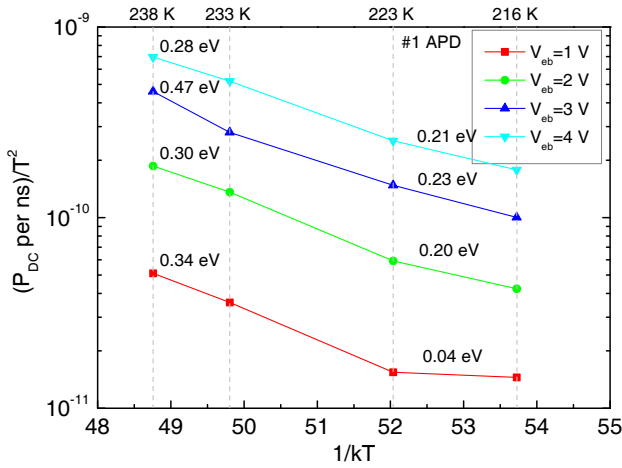


Fig. 6. Plot of P_{DC}/T^2 as a function of $1/kT$ for #1 APD.

The P_{DC} - P_{DE} behavior of #1, #2 and #4 APDs are very similar, with $P_{DC} \sim 1.6 \times 10^{-6} \text{ ns}^{-1}$ and $P_{DE} = 10\%$ at 223 K, as shown in Fig. 4, but much better than #3 APD. Fig. 5 shows the P_{DC} behavior of #2 APD from 210 K to 238 K, and we see a reduction in P_{DC} to $4.5 \times 10^{-7} \text{ ns}^{-1}$ for the same P_{DE} .

The origin of the dark counts is mainly due to the defect concentration in the semiconductor device. There are two main mechanisms for the generation of dark carriers: thermal generation; and tunneling generation. The thermal generation means that a carrier is transferred from the valence band to the conduction band either directly or via the midgap defects, owing to the thermal excitation. Tunneling generation means that a carrier tunnels between the two bands, or it is trapped by a defect first and then tunnels to the conduction band, which is also called trap-assisted tunneling (TAT) [21], [22]. Combinations of the two mechanisms are normally not taken into account. The simulations for $1.06 \mu\text{m}$ InGaAsP/InP APDs performed by Donnelly *et al.* [25] show that TAT in the multiplication layer dominates the P_{DC} at low temperature, while at high temperature the two mechanisms compete with each other. Unfortunately, the dark count model for 1550 nm InGaAs/InP APD is more complicated than this, though one can investigate the so-called thermal activation energy (E_a) to identify the dominant mechanism [19]–[21]. Theoretically, the relationship between P_{DC} , E_a and temperature (T) can be expressed as [20]

$$P_{DC} \propto T^2 e^{-\frac{E_a(T)}{kT}}, \quad (2)$$

where k is the Boltzmann constant and $E_a(T)$ is a function of temperature with slow variations. In Fig. 6, four curves of $\log(P_{DC}/T^2)$ versus $1/kT$ for #1 APD with different V_{eb} values are plotted. We evaluate the difference of E_a values for two small temperature ranges (216 K \sim 223 K and 233 K \sim 238 K). The fitting values are displayed in Fig. 6. The results clearly show that generally higher temperatures induce larger E_a values and suggest that the thermal generation mechanism around 238 K dominates P_{DC} while the TAT mechanism is more significant around 216 K, see also ref. [26].

C. Afterpulsing

During an avalanche process, due to a photon detection, dark count effects, or afterpulsing itself, a carrier can be trapped by a defect in the multiplication layer. This carrier may excite another avalanche - an afterpulse, during subsequent gates. This process severely limits the APD performance for high frequency operation due to the need to apply long, typically $\sim 10 \mu\text{s}$, deadtimes where the APD is inactive. There are two methods to measure the P_{AP} behavior. The first approach measures the total noise behavior as a function of τ_d . When τ_d is large enough, say, $100 \mu\text{s}$, the P_{AP} is negligible and the measured noise is primarily due to dark counts. After subtracting P_{DC} , the quantity of noise left can be attributed to afterpulsing. This method was used in Ref [24] but, while straightforward, generally overestimates P_{AP} .

The other approach, the double-gate method [14], as used in our setup is illustrated in Fig. 2. If there is a click during the detection (AB) gate, the CPLD will also generate an afterpulse (CD) gate after AB's reset pulse with a delay of τ_d to the falling edge of the AB gate. This corresponds to the deadtime. The CPLD also generates a reset pulse for the CD gate only when an afterpulse detection is registered during this gate. This method directly measures P_{AP} .

Assuming a Poisson distribution, P_{AP} can be expressed as

$$P_{AP} = (1 - e^{-R_{AP}(\tau_d)\eta_{av}\tau_{CD}})/\tau_{CD}, \quad (3)$$

where $R_{AP}(\tau_d)$ is the detrapping rate at time τ_d and η_{av} is the avalanche probability. We use a multiple trapping model (multiple detrapping times) to describe $R_{AP}(\tau_d)$ [19], [20],

$$R_{AP}(\tau_d) = \sum_i \frac{N_i}{\Delta t_i} e^{-\tau_d/\Delta t_i}, \quad (4)$$

where N_i is the number of trapped carriers at the end of the detection gate with a detrapping time constant of Δt_i . There are single trapping models that use a single detrapping time constant Δt but in many cases this does not correspond to the measured results. The multiple trapping model effectively fits the measured results but some physical questions remain, e.g., why only 2 detrapping time parameters are needed for modeling one APD while 3 parameters are required for another *etc.* In fact, quantitative description and modeling for P_{AP} behavior is still an intractable problem.

To illustrate the suitability for free-running operations we look at the P_{AP} as we make our detection gates longer. The results for #1 APD are plotted in Fig. 7 and fitted using the multiple trapping model. τ_{CD} is fixed at 100 ns while τ_{AB} and the photon's arrival positions are altered. If the active quenching was slow then the arrival position, or time, of the photon's appearance in the AB gate would be reflected in the P_{AP} behavior. A photon creating an avalanche at the start of a long gate would generate more carriers, increasing the chances for subsequent afterpulses, than in the short gate regime or if the photon arrived at the end of a gate. The overlapping curves show that the P_{AP} behavior doesn't change for long gates, nor is it dependent on the arrival time, and hence shouldn't change when we move to a free-running regime.

We finally study the temperature dependence of afterpulse. The experimental results and fitting curves are shown in Fig. 8

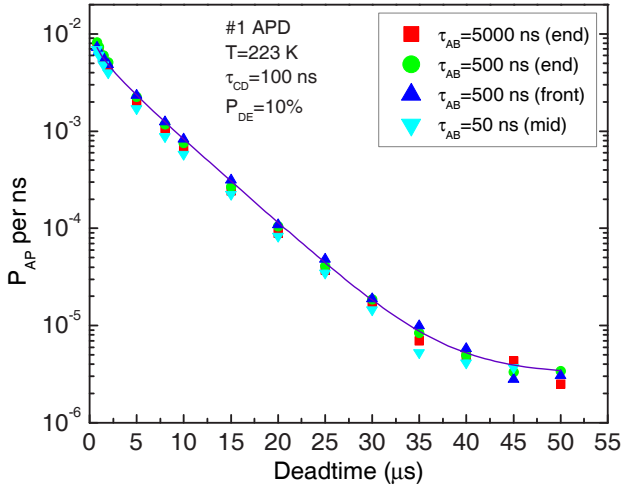


Fig. 7. P_{AP} versus τ_d . “end”, “mid” and “front” mean that incident photons appear in the end, middle and front of AB gates, respectively. The minimum τ_d is always 800 ns in Fig. 7-9.

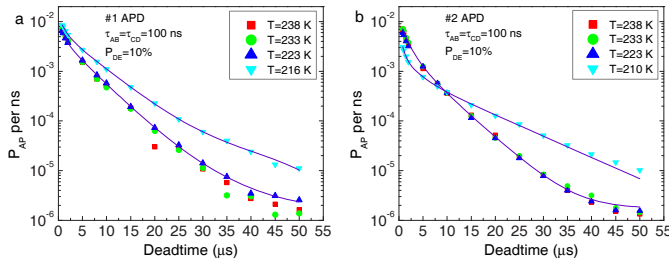


Fig. 8. P_{AP} versus τ_d for #1 (a) and #2 (b) APDs at different T.

TABLE I

THE DETRAPPING TIME PARAMETERS OF FITTING CURVES IN FIG. 8.

APD	T(K)	Δt_1 (ns)	Δt_2 (ns)	Δt_3 (ns)
#1	216	1135	5645	
#1	238-223	860	4385	
#2	210	615	2560	10135
#2	238-223	1020	2165	5075

and the fitting parameters are listed in Table I. When the temperature is varied from 238 K to 223 K the P_{AP} behavior is almost identical due to the close trap lifetime parameters, but when the temperature is at 216 K (#1 APD) or 210 K (#2 APD), there is a distinct increase for the P_{AP} . The detrapping lifetime can be modeled as [27]

$$\Delta t \propto e^{\frac{E_{ta}}{kT}} / T^2, \quad (5)$$

where E_{ta} is the trapping activation energy. This formula means that lower temperatures cause larger Δt for traps, corresponding to larger P_{AP} .

Moreover, when $\tau_d \lesssim 10 \mu s$, the P_{AP} of #2 APD at 210 K, in Fig. 8, is less than at other temperatures, but the P_{AP} of #1 APD at 216 K is not. According to the fitting results at 210 K, there is a trap type with a fast detrapping lifetime of 615 ns in #2 APD, which causes rapid detrapping at small τ_d , but when τ_d becomes large, the effect of this trap type is gradually diminished while the other trap types with 2560 ns and 10135 ns lifetimes start to dominate the detrapping process. Unfortunately, this kind of fast detrapping time is

too short and/or too weak to be measured at the other three temperatures and for #1 APD.

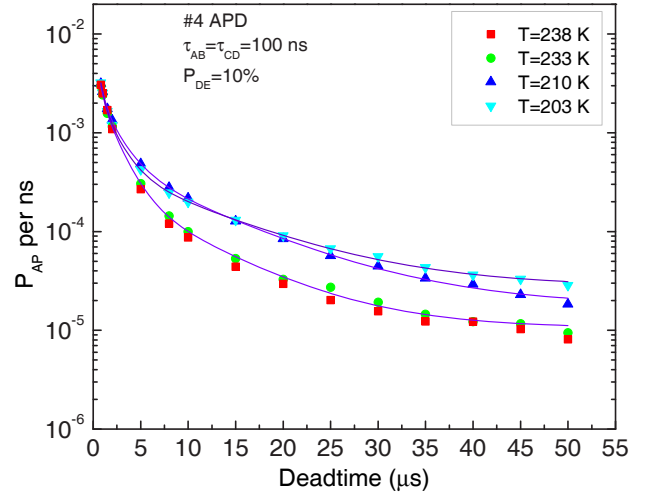


Fig. 9. P_{AP} versus τ_d for #4 APD at different T.

In order to validate the above phenomena, we perform the measurements of P_{AP} behaviors of #4 APD from another manufacturer, whose results are shown in Fig. 9. The P_{AP} increases from 233 K to 210 K while the cross point appears between 210 K to 203 K, which agrees well with our explanation for the different P_{AP} behaviors. We believe that the P_{AP} models so far are not perfect and further investigations, including effective models and experiments, are still needed.

D. Free-running mode

Free-running operation is very important for many applications such as asynchronous and CW photon counting and quantum cryptography [1] *etc.* Due to the lower noise characteristics of InGaAs/InP APDs that use this active quenching ASIC, some of us have recently been able to show that this is now also possible for APDs in the telecom regime.

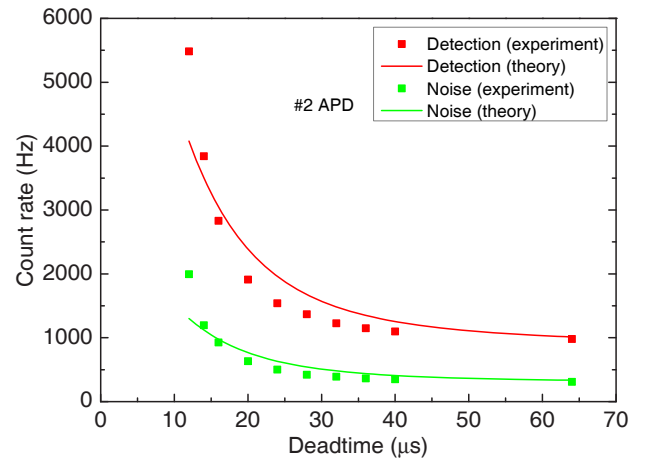


Fig. 10. Plot of the detection and noise rates as a function of deadtime for #2 APD at $V_{DC} = 48.62$ V, $N = 10$ KHz with CW photons and $T = 210$ K, operating in the free-running mode.

As in the gated regime, the operation in the free-running mode depends on the parameters of V_{DC} , τ_d and T. However,

unlike the gated mode, the afterpulse parameter in the free-running mode is more difficult to evaluate.

As we said, with respect to Fig. 7, the P_{AP} does not depend on the width of the gate, which is applicable for the free-running mode. Indeed, it may not be obvious how the afterpulse probability evolves when the gate is open for such long times, though it would appear that at worst, the probability continues to decrease over the period of detection. Nonetheless, we have previously seen that for short deadtimes the afterpulsing dominates [24]. As we have now been able to use the double-gate method to characterize the afterpulsing, in the gated regime, we can use a simple model to describe the detection and noise rates for the free-running mode,

$$R = \eta N(1 - \eta N \tau_d)(1 + \overline{P_{AP}}), \quad (6)$$

with $\eta = 1 - e^{-\mu P_{DE}}(1 - P_{DC})$, considering the Poisson distribution. P_{DE} and P_{DC} are the detection efficiency and dark count probability, and N is the input photon number. The term of $(1 - \eta N \tau_d)$ is for deadtime correction. If we put $\mu = 0$, we recover the noise rate. $\overline{P_{AP}}$ is the total afterpulsing contribution at τ_d , calculated from integrating over the gated afterpulse probability from τ_d to infinity (in practice $100 \mu s$ is sufficient). Fig. 10 shows the experimental rates as well as the results of our model as a function of τ_d .

It is clear that a more complicated model is warranted. However, the physics of these limitations is clear. In the small τ_d region we underestimate the rates as we do not take account of cascaded afterpulses, i.e., higher order effects. The more interesting region, from $20 - 40 \mu s$, we are overestimating due to the difficulty in defining an appropriate integration range, which will also change as a function of the photon flux, the intrinsic detection efficiency and the deadtime. Importantly, we can also conclude that for small τ_d , if N increases, then the $\overline{P_{AP}}$ value will decrease, since photon clicks will increase while the multiple afterpulsing effects will be relatively less likely.

Our model makes a first attempt to both understand the afterpulsing and to develop a reliable technique for determining the detector's characteristics, without resorting to complicated techniques in a double-gate regime, there is still some way to go. Although the apparent need for large τ_d that, in turn, limits the maximum count rate, this is highly dependent on the photon flux to be detected and free-running APDs are certainly highly advantageous for applications with low to moderate count rates.

E. Charge persistence

Charge persistence is not normally a problem for synchronous detectors as the photons arrive during the gate. However, what happens if a photon arrives before the gate is applied, as is possible in the free-running mode, before the APD is activated after a deadtime?

When the detector is "off", i.e., at V_{bv} below V_{br} , with only a few volts so that primary dark carriers can still be generated and multiplied by the average dc gain but with a small probability. When the gate pulse arrives some of the carriers that remained in the multiplication layer can induce

avalanches [28]. This is called "charge persistence" (CP), or sometimes referred as the "twilight effect" [29]. Similarly, when the CP carriers are released before the gate pulses with the time difference less than the effective transit time, they can also create afterpulses [28]. Now let us consider another case, where photons always appear before the gate. Based on the same principle, in this case the number of dark CP carriers will be increased and the CP effect will be expanded.

We experimentally test this effect and the results are shown in Fig. 11. By varying the time difference between the arrival times of gates (T_d) and photons (T_p), we observe the changes of the normalized (for μ) noise per gate, for #4 APD. The two almost identical behaviors show that the CP effect is proportional to photon numbers and, per photon, can generate noise of about 10% of the dark count level with the time difference less than 1 ns. When the time difference is larger than ~ 5 ns, the CP effect is negligible due to the characteristic exponential decrease. Moreover, through using TCSPC, we also observe the detection events at the beginning of the gate are more than those at other regions. The CP effect will cause nonnegligible noise in the case of high frequency gating or asynchronous high flux detection.

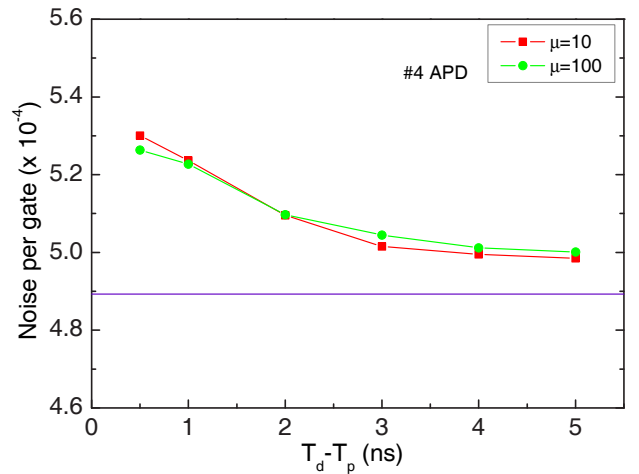


Fig. 11. The noise, including CP and dark counts per gate, normalized by μ , as a function of time difference between detection gate (T_d) and photons (T_p). The horizontal line is the dark count level. The results are tested using #4 APD at $P_{DE}=10\%$.

F. Quenching time

Quantifying the quenching time, including the circuit reaction time and gate closing time as shown in Fig. 12, of an avalanche is very important to understand the avalanche dynamics of APDs. Although an active quenching ASIC should have a faster quenching time than conventional electronics this has not previously been measured. More generally, these results are also pertinent for rapid gating schemes that use very short gates and hence terminate avalanches very quickly.

The principle for measuring the quenching time is to compare the count rate behaviors for detections and afterpulses, see Fig. 12, using the double-gate measurement electronics. The total number of carriers, during an avalanche, should be proportional to the excess bias on APD and the excess bias

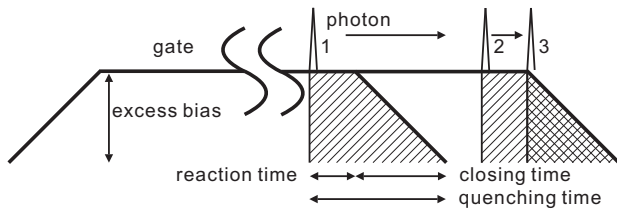


Fig. 12. The principle of measuring the quenching time.

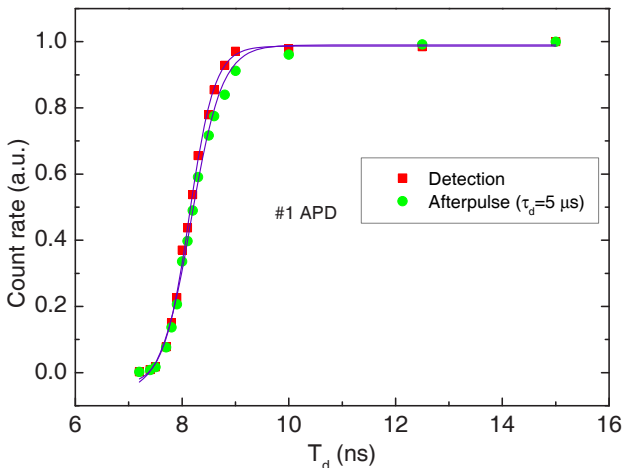


Fig. 13. The count rates of detections and afterpulses with $\tau_d = 5 \mu s$ versus the delay of detection gate (T_d). Points and lines are experimental values and theoretical S fits, respectively. The results are tested with #1 APD at $T = 223$ K and $P_{DE} = 10\%$.

duration, or the integral of excess bias over the quenching time. Now we consider the case where photons arrive at the end of the detection gates, by delaying photons. From phase 1 to phase 2 in Fig. 12, the count rates of detection and afterpulse are both almost constant, while from phase 2 to phase 3 the detection rate is still constant but the afterpulse rate decreases first due to the decrease of the integral. The time difference between the two phases can be regarded as the reaction time, to detect the onset of the avalanche and send the signal to close the NMOS switch. After phase 3, both of the rates drastically decrease until the end of the closing time.

Fig. 13 shows the results of these measurements on #1 APD. From the slope of the detection rate, we can obtain the closing time of the gate, which is only around 1 ns. Although it is very hard to determine a precise value of the reaction time from the fitting results, the slight shift between the detection and afterpulse rates indicates that the reaction time is much less than the closing time.

IV. CONCLUSION

In summary, we have fully characterized an active quenching ASIC and compared its operation with a conventional electronic circuit. To show the improvements are universal we also characterized and compared 4 different InGaAs/InP APDs. The APDs operating in the gated mode exhibit substantial performance improvements compared with the conventional quenching electronics and allow for free-running operation. We also extract thermal activation energies to identify the

dominant mechanism of dark counts, and by employing the multiple detrapping model in the gated mode and proposed model in the free-running mode the afterpulse behaviors are well illustrated. Moreover, we have characterized the charge persistence and quenching time. The advantages of low afterpulsing and noise in both these regimes are mostly attributed to the state-of-the-art ASIC.

ACKNOWLEDGMENT

The authors would like to thank Dr. A. Rochas and Dr. M. A. Itzler for useful discussions.

REFERENCES

- [1] N. Gisin, G. Ribordy, W. Tittel, and H. Zbinden, "Quantum cryptography," *Rev. Mod. Phys.*, vol. 74, pp. 145-195, Jan. 2002.
- [2] B. F. Levine, C. G. Bethea, and J. Campbell, "1.52 μm room temperature photon counting optical time domain reflectometer," *Electron. Lett.*, vol. 21, no. 5, pp. 194-196, Feb. 1985.
- [3] M. Wegmuller, F. Scholder, and N. Gisin, "Photon-Counting OTDR for local birefringence and fault analysis in the metro environment," *J. Lightwave Technol.*, vol. 22, no. 2, pp. 390-400, Feb. 2004.
- [4] F. Stellari, P. Song, J.C. Tsang, M.K. McManus, and M.B. Ketchen, "Testing and diagnostics of CMOS circuits using light emission from off-state leakage current," *IEEE Trans. on Electron Devices*, vol. 51, no. 9, pp. 1455-1462, Sep. 2004.
- [5] *Photomultiplier Tubes: Basics and Applications (3rd Edition)*. Hamamatsu Photonics, Hamamatsu City, Japan, 2006.
- [6] S. Cova, M. Ghioni, A. L. Lacaita, C. Samori, and F. Zappa, "Avalanche photodiodes and quenching circuits for single-photon detection," *Appl. Opt.*, vol. 35, no. 12, pp. 1956-1976, Apr. 1996.
- [7] J.C. Campbell, S. Demiguel, F. Ma, A. Beck, X. Guo, S. Wang, X. Zheng, X. Li, J.D. Beck, M.A. Kinch, A. Huntington, L.A. Coldren, J. Decobert, N. Tschertner, "Recent advances in avalanche photodiodes," *IEEE J. Sel. Top. Quantum Electron.*, vol. 10, no. 4, pp. 777-787, Jul. 2004.
- [8] G. N. Gol'tsman, O. Okunev, G. Chulkova, A. Lipatov, A. Semenov, K. Smirnov, B. Voronov, A. Dzardanov, C. Williams, and R. Sobolewski, "Picosecond superconducting single-photon optical detector," *Appl. Phys. Lett.*, vol. 79, no.6, pp. 705-707, Aug. 2001.
- [9] S. Komiyama, O. Astafiev, V. Antonov, T. Kutsuwa, and H. Hirai, "A single-photon detector in the far-infrared range," *Nature (London)*, vol. 403, pp. 405-407, Jan. 2000.
- [10] A. Lacaita, F. Zappa, S. Cova, and P. Lovati, "Single-photon detection beyond 1 μm : performance of commercially available InGaAs/InP detectors," *Appl. Opt.*, vol. 35, no. 16, pp. 2986-2996, Jun. 1996.
- [11] G. Ribordy, J.-D. Gautier, H. Zbinden, and N. Gisin, "Performance of InGaAs/InP avalanche photodiodes as gated-mode photon counters," *Appl. Opt.*, vol. 37, no. 12, pp. 2272-2277, Apr. 1998.
- [12] J. G. Rarity, T. E. Wall, K. D. Ridley, P. C. M. Owens, and P. R. Tapster, "Single-photon counting for the 1300-1600-nm range by use of Peltier-cooled and passively quenched InGaAs avalanche photodiodes," *Appl. Opt.*, vol. 39, no. 36, pp. 6746-6753, Dec. 2000.
- [13] P. A. Hiskett, G. S. Buller, A. Y. Loudon, J. M. Smith, I. Gontijo, A. C. Walker, P. D. Townsend, and M. J. Robertson, "Performance and Design of InGaAs /InP Photodiodes for Single-Photon Counting at 1.55 μm ," *Appl. Opt.*, vol. 39, no. 36, pp. 6818-6829, Dec. 2000.
- [14] D. Stucki, G. Ribordy, A. Stefanov, H. Zbinden, J. G. Rarity, and T. Wall, "Photon counting for quantum key distribution with Peltier cooled InGaAs/InP APDs," *J. Mod. Opt.*, vol. 48, no. 13, pp. 1967-1981, Nov. 2001.
- [15] G. Karve, X. Zheng, X. Zhang, X. Li, N. Li, S. Wang, F. Ma, A. Holmes, J. C. Campbell, G. S. Kinsey, J. C. Boisvert, T. D. Isshiki, R. Sudharsanan, D. S. Bethune, and W. P. Risk, "Geiger mode operation of an $In_{0.53}Ga_{0.47}As - In_{0.52}Al_{0.48}As$ avalanche photodiode," *IEEE J. Quantum Electron.*, vol. 39, no. 10, pp. 1281-1286, Oct. 2003.
- [16] G. Ribordy, N. Gisin, O. Guinnard, D. Stucki, M. Wegmuller, and H. Zbinden, "Photon counting at telecom wavelengths with commercial InGaAs/InP avalanche photodiodes: Current performance," *J. Mod. Opt.*, vol. 51, pp. 1381-1398, Jun. 2004.

- [17] D. A. Ramirez, M. M. Hayat, G. Karve, J. C. Campbell, S. N. Torres, B. E. A. Saleh, and M. C. Teich, "Detection efficiencies and generalized breakdown probabilities for nanosecond-gated near infrared single-photon avalanche photodiodes," *IEEE J. Quantum Electron.*, vol. 42, no. 2, pp. 137-145, Feb. 2006.
- [18] S. Pellegrini, R. E. Warburton, L. J. J. Tan, J. S. Ng, A. B. Krysa, K. Groom, J. P. R. David, M. J. Robertson, and G. S. Buller, "Design and performance of an InGaAs-InP single-photon avalanche diode detector," *IEEE J. Quantum Electron.*, vol. 42, no. 4, pp. 397-403, Apr. 2006.
- [19] M. A. Itzler, R. Ben-Michael, C.-F. Hsu, K. Slomkowski, A. Tosi, S. Cova, F. Zappa, and R. Ispasoiu, "Single photon avalanche diodes (SPADs) for 1.55 μm photon counting applications," *J. Mod. Opt.*, vol. 54, no. 2-3, pp. 283-304, Feb. 2007.
- [20] M. Liu, C. Hu, X. Bai, X. Guo, J. C. Campbell, Z. Pan, and M. M. Tashima, "High-performance InGaAs/InP single-photon avalanche photodiode," *IEEE J. Sel. Top. Quantum Electron.*, vol. 13, no. 4, pp. 887-894, Jul. 2007.
- [21] X. Jiang, M. A. Itzler, R. Ben-Michael, and K. Slomkowski, "InGaAsP-InP avalanche photodiodes for single photon detection," *IEEE J. Sel. Top. Quantum Electron.*, vol. 13, no. 4, pp. 895-905, Jul. 2007.
- [22] X. Jiang, M. A. Itzler, R. Ben-Michael, and K. Slomkowski, M. A. Krainak, S. Wu, and X. Sun, "Afterpulsing Effects in Free-Running InGaAsP Single-Photon Avalanche Diodes," *IEEE J. Quantum Electron.*, vol. 44, no. 1, pp. 3-11, Jan. 2008.
- [23] A. Rochas, C. Guillaume-Gentil, J.-D. Gautier, A. Pauchard, G. Ribordy, H. Zbinden, Y. Leblebici, and L. Monat, "ASIC for high speed gating and free running operation of SPADs," *Proc. SPIE*, vol. 6583, pp. 65830F-1-65830F-10, May. 2007.
- [24] R. T. Thew, D. Stucki, J.-D. Gautier, H. Zbinden, and A. Rochas, "Free-running InGaAs/InP avalanche photodiode with active quenching for single photon counting at telecom wavelengths," *Appl. Phys. Lett.*, vol. 91, no. 20, pp. 201114-1-201114-3, Nov. 2007.
- [25] J. P. Donnelly, E. K. Duerr, K. A. McIntosh, E. A. Dauler, D. C. Oakley, S. H. Groves, C. J. Vineis, L. J. Mahoney, K. M. Molvar, P. I. Hopman, K. E. Jensen, G. M. Smith, S. Verghese, and D. C. Shaver, "Design considerations for 1.06 μm InGaAsP-InP Geiger-mode avalanche photodiodes," *IEEE J. Quantum Electron.*, vol. 42, no. 8, pp. 797-809, Aug. 2006.
- [26] M. A. Itzler, R. Ben-Michael, X. Jiang, and K. Slomkowski, "Geiger-Mode Avalanche Photodiodes for Near-Infrared Photon Counting," in *Conference on Lasers and Electro-Optics/Quantum Electronics and Laser Science Conference and Photonic Applications Systems Technologies*, OSA Technical Digest Series (CD) (Optical Society of America, 2007), paper CMI1.
- [27] K. E. Jensen, P. I. Hopman, E. K. Duerr, E. A. Dauler, J. P. Donnelly, S. H. Groves, L. J. Mahoney, K. A. McIntosh, K. M. Molvar, A. Napoleone, D. C. Oakley, S. Verghese, C. J. Vineis, and R. D. Younger, "Afterpulsing in Geiger-mode avalanche photodiodes for 1.06 μm wavelength," *Appl. Phys. Lett.*, vol. 88, no. 13, pp. 133503-1-133503-3, Mar. 2006.
- [28] Y. Kang, H. X. Lu, Y.-H. Lo, D. S. Bethune, and W. P. Risk, "Dark count probability and quantum efficiency of avalanche photodiodes for single-photon detection," *Appl. Phys. Lett.*, vol. 83, no. 14, pp. 2955-2957, Oct. 2003.
- [29] S. V. Polyakov and A. L. Migdall, "High accuracy verification of a correlated-photon-based method for determining photoncounting detection efficiency," *Opt. Express*, vol. 15, no. 4, pp. 1390-1407, Feb. 2007.